

Equation of state of a seven-dimensional hard-sphere fluid

Miguel Robles* and Mariano López de Haro†

Centro de Investigación en Energía, UNAM, Temixco, Morelos 62580, Mexico

Andrés Santos‡

Departamento de Física, Universidad de Extremadura, E-06071 Badajoz, Spain

(Dated: May 22, 2019)

Following the work of Leutheusser [Physica A **127**, 667 (1984)], the analytical solution to the Percus–Yevick equation for a seven-dimensional hard-sphere fluid is explicitly found. This allows the derivation of the equation of state for the fluid taking both the virial and the compressibility routes. An analysis of the virial coefficients and the determination of the radius of convergence of the virial series are carried out. Molecular dynamics simulations of the same system are also performed and a comparison between the simulation results for the compressibility factor and theoretical expressions for the same quantity is presented.

I. INTRODUCTION

In liquid theory there has been a long lasting interest on the equilibrium properties of high-dimensional hard-sphere fluids, especially in the last few years.^{1,2,3,4,5,6,7,8,9,10,11,12,13,14,15,16,17,18,19,20,21,22,23,24,25,26} Such an interest has arisen from many different sources. To begin with, given the relative simplicity of the intermolecular interactions in these hard-core systems, they are amenable to both theoretical and computer simulation studies. In this sense and as it occurs in other problems in theoretical and mathematical physics, it is an asset that one can deal with hard spheres in arbitrary dimensionality and exploit some of the features that these systems have in common, for instance the fact that they all exhibit a first-order freezing transition. Furthermore, and as pointed out neatly by Frisch and Percus,¹⁵ in the case of fluids high spatial dimensionality has a parallel with limiting high density situations. Therefore one expects that by increasing the dimensionality one may obtain at least a rough idea of any thermodynamic phenomenology that extends to such dimensionality, on the grounds that explicit calculations usually become simpler. An example of this expectation is the recent investigation of the demixing problem in mixtures of hard hyperspheres.¹⁸

Computer simulation studies of hard-sphere fluids in dimensions greater than three are very scarce. To the best of our knowledge, only the four- and five-dimensional simple^{5,11} and multicomponent²¹ fluids have been simulated. This is not surprising since the computational effort needed to obtain reliable results increases significantly with the dimensionality.

Exact information on the equation of state (EOS) usually comes from the virial coefficients B_n defined by²⁷

$$\begin{aligned} Z \equiv \frac{p}{\rho k_B T} &= 1 + \sum_{n=2}^{\infty} B_n \rho^{n-1} \\ &= 1 + \sum_{n=2}^{\infty} b_n \eta^{n-1}. \end{aligned} \quad (1)$$

In this equation, p is the pressure, ρ is the number density, k_B is the Boltzmann constant, T is the temperature, and Z is the compressibility factor. The second virial coefficient is $B_2 = 2^{d-1} v_d \sigma^d$, where d is the dimensionality, σ is the diameter of a sphere, and $v_d = (\pi/4)^{d/2} / \Gamma(1 + d/2)$ is the volume of a d -dimensional sphere of unit diameter. In the second line of Eq. (1) we have introduced the packing fraction $\eta \equiv \rho v_d \sigma^d$ and the reduced virial coefficients $b_n \equiv B_n / (v_d \sigma^d)^{n-1} = 2^{(d-1)(n-1)} B_n / B_2^{n-1}$. The radius of convergence of the virial series (1), $\rho_{\text{conv}} = \lim_{n \rightarrow \infty} |B_n / B_{n+1}|$, is the modulus of the singularity of $Z(\rho)$ closest to the origin in the complex ρ plane. If such a singularity were located on the positive real axis, then all the virial coefficients B_n would be positive for large n .

The exact expression for the third virial coefficient is^{2,7}

$$\frac{B_3}{B_2^2} = 2 \frac{B_{3/4}(d/2 + 1, 1/2)}{B(d/2 + 1/2, 1/2)}, \quad (2)$$

where $B(a, b) = \Gamma(a)\Gamma(b)/\Gamma(a + b)$ is the beta function and $B_x(a, b)$ is the incomplete beta function. Both B_2 and B_3 are positive definite for arbitrary d . The analytic evaluation of the fourth virial coefficient is much more involved. Luban and Baram^{2,3} derived exact expressions for two of the three terms contributing to B_4 and proposed a semi-empirical formula for the remaining contribution. More recently, Clisby and McCoy^{24,26} showed that B_4 can be evaluated exactly for any *even* dimension d and gave the explicit results for $d = 4, 6, 8, 10$, and 12. They also

computed numerically^{25,26} the fifth and sixth virial coefficients through $d = 50$. The results show that, while B_5 remains positive, B_4 and B_6 become negative for $d \geq 8$ and $d \geq 6$, respectively. This suggests the possibility that, even in the three-dimensional case, there might be negative virial coefficients B_n for sufficiently large n . The fact that the virial coefficients are not positive definite and that they may have alternate signs is of importance in connection with the radius of convergence of the virial expansion (1), as mentioned before.

Frisch and Percus¹⁵ analyzed by means of asymptotic methods and heuristic arguments the situation in the limit of high dimensionality. Their analysis leads to the following scenario in that limit:

- The fourth virial coefficient is negative. Beyond that term, the virial expansion is an alternating series.
- The virial series is convergent for $\hat{\rho} < 1$, where $\hat{\rho} \equiv 2\eta^{1/d}$ is the scaled density per dimension. In terms of the packing fraction, the virial series converges for $\eta < \eta_{\text{conv}} = 2^{-d}$.
- In the density range $\hat{\rho} < 1$ the second virial term dominates over the remaining ones, so that

$$Z \approx 1 + B_2\rho = 1 + \frac{\hat{\rho}^d}{2}. \quad (3)$$

- Even though the virial expansion does not converge for $\hat{\rho} > 1$ (oscillatory divergence), the truncated series (3) remains valid within the interval $1 < \hat{\rho} < (1 - \epsilon)\hat{\rho}_0$, where $\epsilon = \mathcal{O}(d^{-1})$ and

$$\hat{\rho}_0 = \left(1.148d^{-1/6}e^{-1.473d^{1/3}}\right)^{-1/d} \sqrt{e/2} \sim \sqrt{e/2} \simeq 1.17. \quad (4)$$

- At the density $\hat{\rho} = \hat{\rho}_0$ an infinite compressibility spinodal appears, thus indicating a first-order transition to the high-dimensional solid.

In an independent paper, Parisi and Slanina¹⁹ reached similar conclusions from a toy model based on simplified HNC equations. They obtained that, while in the limit $d \rightarrow \infty$ the EOS for $\hat{\rho} < 1$ is given by Eq. (3), in the interval $1 < \hat{\rho} < \hat{\rho}_0 = \sqrt{e/2}$, one has

$$Z(\hat{\rho}) = 1 + \hat{\rho}^d \left[\frac{1}{2} + \Delta(\hat{\rho}) \right], \quad (5)$$

where

$$\Delta(\hat{\rho}) = \left[\frac{e\kappa(\hat{\rho})}{2\hat{\rho}^2} \right]^d, \quad (6)$$

$\kappa(\hat{\rho})$ being the solution to²⁸

$$\ln \frac{2\hat{\rho}^2}{e} = \ln \left(1 + \sqrt{1 - \kappa^2} \right) - \sqrt{1 - \kappa^2}. \quad (7)$$

Note that, since $\ln \kappa < \ln \left(1 + \sqrt{1 - \kappa^2} \right) - \sqrt{1 - \kappa^2}$ for $0 < \kappa < 1$, one has $\lim_{d \rightarrow \infty} \Delta(\hat{\rho}) = 0$ for $\hat{\rho} < \hat{\rho}_0$. Although, strictly speaking, Eq. (7) cannot be extended to $\hat{\rho} > \hat{\rho}_0$, Eq. (6) suggests that $\lim_{d \rightarrow \infty} \Delta(\hat{\rho}) = \infty$ in that density domain, in agreement with the phase transition noted by Frisch and Percus.²⁹

As in two and three dimensions, one can make use of approximate schemes to represent the EOS of hard hyperspheres. Several proposals have been made in the literature for the EOS based on the knowledge of the first few virial coefficients.^{7,8,9,10,13} For illustration, we review here a few of them making use of the first three virial coefficients. The extension to higher virial coefficients is straightforward. The first obvious choice is the truncated virial expansion

$$Z_{[2,0]}(\eta) = 1 + b_2\eta + b_3\eta^2. \quad (8)$$

As discussed above, this simple approximation becomes more and more accurate in the stable fluid domain as the dimensionality increases. In a way analogous to Eq. (8) it is possible to define a truncated expansion $Z_{[n,0]}$ from the knowledge of the first $n + 1$ virial coefficients. One can also construct Padé approximants of the form $Z_{[m,n]}$ from the first $n + m + 1$ virial coefficients. For instance,

$$Z_{[1,1]}(\eta) = \frac{b_2 + (b_2^2 - b_3)\eta}{b_2 - b_3\eta}, \quad (9)$$

$$Z_{[0,2]}(\eta) = [1 - b_2\eta + (b_2^2 - b_3)\eta^2]^{-1}. \quad (10)$$

Colot and Baus^{6,7} proposed (truncated) *rescaled* virial expansions, where the series expansion of $(1 - \eta)^d Z(\eta)$, rather than that of $Z(\eta)$, is truncated. Let us denote by $Z_{[n,0]}^{\text{BC}}(\eta)$ the truncated rescaled virial expansion that makes use of the first $n + 1$ virial coefficients. For example,

$$Z_{[2,0]}^{\text{BC}}(\eta) = \frac{1 + (b_2 - d)\eta + [b_3 - b_2d + d(d - 1)/2]\eta^2}{(1 - \eta)^d}. \quad (11)$$

The pole of order d at the (unphysical) density $\eta = 1$ is suggested by the scaled particle theory. Maeso et al.¹³ combined the advantages of Padé approximants and rescaled expansions by proposing Padé approximants for $(1 - \eta)^d Z(\eta)$. A rescaled Padé approximant constructed from the first $n + m + 1$ virial coefficients will be denoted here as $Z_{[m,n]}^{\text{MSAV}}(\eta)$. Thus,

$$Z_{[1,1]}^{\text{MSAV}}(\eta) = \frac{1}{(1 - \eta)^d} \frac{b_2 - d + [d(d + 1)/2 + b_2(b_2 - d) - b_3]\eta}{b_2 - d - [b_3 - b_2d + d(d - 1)/2]\eta}. \quad (12)$$

By construction, $Z_{[n,0]}^{\text{MSAV}}(\eta) = Z_{[n,0]}^{\text{BC}}(\eta)$. Using simple arguments, Song et al.^{8,10} proposed the following generalization to d dimensions of the celebrated Carnahan–Starling (CS) EOS for three-dimensional hard spheres:³⁰

$$Z_{\text{SMS}}(\eta) = 1 + b_2\eta \frac{1 + (b_3/b_2 - d)\eta}{(1 - \eta)^d}. \quad (13)$$

On a different vein, Luban and Michels¹¹ wrote the compressibility factor as

$$Z_{\text{LM}}(\eta) = 1 + b_2\eta \frac{1 + [b_3/b_2 - \zeta(\eta)b_4/b_3]\eta}{1 - \zeta(\eta)(b_4/b_3)\eta + [\zeta(\eta) - 1](b_4/b_2)\eta^2}. \quad (14)$$

The knowledge of the function $\zeta(\eta)$ is equivalent to that of $Z(\eta)$. However, $\zeta(\eta)$ focuses on the high density behavior of the EOS, since Eq. (14) is consistent with the exact first four virial coefficients, regardless of the choice of $\zeta(\eta)$. The approximation $\zeta(\eta) = 1$ is equivalent to assuming a Padé approximant $Z_{[2,1]}(\eta)$. Instead, Luban and Michels observed that the computer simulation data for $d = 2$ –5 favor a *linear* approximation $\zeta(\eta) = a + b\eta$, with coefficients obtained by a least-square fit to the simulation results for each dimensionality.

It is noteworthy that the Percus–Yevick (PY) integral equation can be solved analytically in odd dimensions, as first pointed out by Freasier and Isbister¹ and, independently, Leutheusser.⁴ In general, the problem reduces to an algebraic equation of degree $d - 3$. In five dimensions, one has to deal with a quadratic equation^{1,4} and explicit expressions for the virial and compressibility routes to the EOS can be obtained.¹⁶ A simple analysis of the solution shows that the virial route incorrectly gives a negative value for B_6 : $B_6^{\text{PY-v}}/B_2^5 = -\frac{2999}{16^5} \simeq -0.00286$. The compressibility route yields $B_6^{\text{PY-c}}/B_2^5 = \frac{12233}{8 \times 16^5} \simeq 0.00146$, while the correct value is $B_6/B_2^5 \simeq 0.00094$.^{25,26} Both routes consistently predict that B_8 is negative, with subsequent coefficients alternating in sign. On the other hand, the virial route gives values for the magnitude of B_n ($n \geq 8$) increasingly larger than the compressibility route: $B_n^{\text{PY-v}}/B_n^{\text{PY-c}} \approx 0.66 + 0.77n$. The alternating character of the virial series predicted by the PY equation for $d = 5$ is due to a branch singularity located on the *negative* real axis at $\eta_{\text{branch}} = -(9 - 5\sqrt{3})/6 \simeq -0.0566243$. The radius of convergence $\eta_{\text{conv}}^{\text{PY}} \simeq 0.0566243$ of the PY solution for $d = 5$ is larger than the value $2^{-5} = 0.03125$ extrapolated from the radius $\lim_{d \rightarrow \infty} \eta_{\text{conv}} = 2^{-d}$, but is close to the estimate $\eta_{\text{conv}} \simeq 0.052$ made by Clisby and McCoy on the basis of Monte Carlo evaluation of sets of Ree–Hoover diagrams.^{25,26} All these estimates are sensibly smaller than the packing fraction $\eta_f = 0.19$ at which freezing occurs for $d = 5$.^{5,11,22}

As is well known, the CS EOS for three-dimensional hard spheres can be interpreted as a weighted average between the PY virial and compressibility routes:

$$Z_{\text{CS}}(\eta) = \alpha Z_{\text{PY-c}}(\eta) + (1 - \alpha) Z_{\text{PY-v}}(\eta), \quad (15)$$

where $\alpha = \frac{2}{3}$. Given that the PY equation can be solved for odd dimensions, It is then natural to speculate about whether or not the prescription (15), with an adequate choice of the mixing parameter α , keeps being reliable for $d > 3$, even though the internal inconsistency between both routes seems to increase dramatically with the dimensionality.¹ In the five-dimensional case, one of us¹⁷ showed that the choice $\alpha = \frac{3}{5}$ leads to values of Z_{CS} in excellent agreement with computer simulations.⁵ This suggested that the choice $\alpha = (d + 1)/2d$ might provide a good description for

$d \geq 3$. Note that, while Eqs. (13) and (15) coincide at $d = 3$, they differ for $d > 3$, so they generalize the original CS EOS along different directions. An alternative generalization of the CS EOS was made by Gonzalez et al.¹² They proposed a simple ansatz for the direct correlation function $c(r)$, which reduced exactly to the PY theory for $d = 1$ and $d = 3$ and gave results very close to the PY theory for other dimensions. Their generalized CS EOS consisted of a weighted average between the virial and compressibility routes obtained from their theory with a mixing parameter $\alpha = 2(2d - 1)/5d$.

The aim of this paper is threefold. First, we present the explicit *analytic* solution to the PY equation in the case of a seven-dimensional hard-sphere fluid following the procedure introduced by Leutheusser.⁴ This allows us to derive the EOS of the fluid both through the virial and the compressibility routes, as well as to analyze the behavior of the virial coefficients stemming out of them. Secondly, we provide molecular dynamics results for the compressibility factor. And finally we perform a comparison between different proposals for the EOS of a seven-dimensional hard-sphere fluid with the simulation data.

The paper is organized as follows. In Section II we provide the analytic solution of the PY equation for a seven-dimensional hard-sphere fluid as well as the analysis of the virial coefficients arising from the derivation of the EOS using the virial and the compressibility routes. This is followed in Section III by a description of the molecular dynamics simulation that was carried out to obtain the compressibility factor of the fluid. The results of the simulation are then used to assess the merits of various proposals that have been made in the literature for the EOS. The paper is closed in Section IV with further discussion of the results and some concluding remarks.

II. SOLUTION OF THE PERCUS–YEVICK EQUATION FOR A SEVEN-DIMENSIONAL HARD-SPHERE FLUID

As mentioned in Sec. I, the solution to the PY equation for hard hyperspheres with $d = \text{odd}$ reduces to an algebraic equation of degree $d - 3$.^{1,4} The highest dimensionality for which the algebraic problem lends itself to an analytic solution is $d = 7$. Here we sketch the solution for such a case. For simplicity, in the remainder of this Section we set $\sigma = 1$.

In the Percus–Yevick approximation, the structure factor $S(q)$ of a hard-sphere fluid in $d = 2k + 1$ dimensions is

$$S(q) = \frac{1}{\tilde{Q}(q)\tilde{Q}(-q)}, \quad (16)$$

where

$$\tilde{Q}(q) = 1 - \lambda \int_0^1 dr e^{iqr} Q(r), \quad \lambda \equiv (2\pi)^k \rho = 2^{2k} (2k + 1)!! \eta, \quad (17)$$

$Q(r)$ having the form

$$Q(r) = \begin{cases} \sum_{m=0}^k Q_m (r - 1)^{m+k}, & 0 \leq r \leq 1, \\ 0, & r \geq 1. \end{cases} \quad (18)$$

The $k + 1$ coefficients $\{Q_m\}$ are functions of the density determined by the two linear equations

$$(-1)^k = -k! 2^k Q_k + \lambda \sum_{m=0}^k (-1)^m \frac{Q_m}{k + m + 1}, \quad k \geq 0, \quad (19)$$

$$(-1)^k = -(k - 1)! 2^{k-1} Q_{k-1} + \lambda \sum_{m=0}^k (-1)^m \frac{Q_m}{k + m + 2}, \quad k \geq 1, \quad (20)$$

plus the $k - 1$ nonlinear equations

$$Q^{(2m+1)}(0) = \frac{1}{2} \lambda (-1)^{m+1} \left[Q^{(m)}(0) \right]^2 - \lambda \sum_{\nu=0}^{m-1} (-1)^\nu Q^{(\nu)}(0) Q^{(2m-\nu)}(0), \quad 0 \leq m \leq k - 2. \quad (21)$$

Here $Q^{(\nu)}(r)$ represents the ν -th derivative of the function $Q(r)$. For $k = 0$ ($d = 1$), Eq. (19) gives the exact solution for hard rods. For $k = 1$ ($d = 3$), Eqs. (19) and (20) are sufficient to find the solution of the PY equation. However,

for $k \geq 2$ ($d \geq 5$) one needs in addition Eq. (21), so that the problem reduces to solving an algebraic equation of degree $2(k-1) = d-3$.

In the limit $\eta \rightarrow 0$, it is easy to verify that

$$\lim_{\eta \rightarrow 0} Q_m = (-1)^{k+1} \frac{2^{-m}}{k!} \binom{k}{m}, \quad \lim_{\eta \rightarrow 0} Q(r) = (-1)^{k+1} \frac{2^{-k}}{k!} (r^2 - 1)^k, \quad (22)$$

$$\lim_{\eta \rightarrow 0} Q^{(2m)}(0) = (-1)^{m+1} 2^{-k} \frac{(2m)!}{m!(k-m)!}, \quad \lim_{\eta \rightarrow 0} Q^{(2m+1)}(0) = 0. \quad (23)$$

In general, one can expand the coefficients Q_m in powers of η :

$$Q_m(\eta) = \sum_{n=0}^{\infty} Q_{m,n} \eta^n, \quad (24)$$

where $Q_{m,0}$ is given by the first equation of (22). Of course, the full nonlinear dependence of the coefficients $Q_m(\eta)$ can be obtained from the solution to the set of equations (19)–(21), either analytically ($k \leq 3$) or numerically ($k \geq 4$).

Once one has determined the function $Q(r)$, the structural properties of the fluid are given by Eqs. (16) and (17). In particular, the long wavelength limit of the structure factor is

$$S(q=0) = \frac{1}{[k!2^k Q_k]^2}. \quad (25)$$

The contact value of the radial distribution function is

$$g(1^+) = (-1)^{k+1} k! Q_0. \quad (26)$$

The virial route to the EOS is given by

$$Z = 1 + 2^{d-1} \eta g(1^+), \quad (27)$$

while the compressibility route is

$$\chi \equiv k_B T \left(\frac{\partial \rho}{\partial p} \right)_T = S(q=0). \quad (28)$$

Inserting the expansion (24) into Eqs. (27) and (28) we get the virial coefficients along both routes:

$$b_{n+2}^{\text{PY-v}} = 2^{2k} (-1)^{k+1} k! Q_{0,n}, \quad b_{n+1}^{\text{PY-c}} = 2^{2k} (k!)^2 \frac{1}{n+1} \sum_{m=0}^n Q_{k,m} Q_{k,n-m}. \quad (29)$$

In the seven-dimensional case ($k=3$) the unknowns are Q_m , $m=0, 1, 2, 3$. Since the two nonlinear equations (21) involve the derivatives $Q^{(m)} \equiv Q^{(m)}(0)$, it is more advantageous to work with the set $\{Q^{(m)}\}$ rather than with the set $\{Q_m\}$. The latter can be expressed in terms of the former as

$$\begin{pmatrix} Q_0 \\ Q_1 \\ Q_2 \\ Q_3 \end{pmatrix} = - \begin{pmatrix} 20 & 10 & 2 & \frac{1}{6} \\ 45 & 25 & \frac{11}{2} & \frac{1}{2} \\ 36 & 21 & 5 & \frac{1}{3} \\ 10 & 6 & \frac{3}{2} & \frac{1}{6} \end{pmatrix} \cdot \begin{pmatrix} Q^{(0)} \\ Q^{(1)} \\ Q^{(2)} \\ Q^{(3)} \end{pmatrix}. \quad (30)$$

Equations (19) and (20), plus Eq. (21) with $m=0$ yield

$$Q^{(1)} = -3360\eta Q^{(0)2}, \quad (31)$$

$$Q^{(2)} = - \frac{1 + 96Q^{(0)} \{1 - 5\eta [3 + 112Q^{(0)}(3 - 10\eta)]\}}{8(1 - \eta)}, \quad (32)$$

TABLE I: Values of $Q_{m,n}$ for $n = 0-6$.

n	$Q_{0,n}$	$Q_{1,n}$	$Q_{2,n}$	$Q_{3,n}$
0	0.166666667	0.250000000	0.125000000	0.020833333
1	3.010416667	7.888020833	5.812500000	1.333333333
2	-5.119791667	-59.313802083	-41.072916667	-6.541666667
3	5.395897352×10^2	4.247567790×10^3	3.201932292×10^3	6.540590278×10^2
4	-2.286456505×10^4	-2.488562475×10^5	-1.884527380×10^5	-3.841568446×10^4
5	1.172728501×10^6	1.635350292×10^7	1.241794603×10^7	2.538798289×10^6
6	-6.600274174×10^7	-1.143524052×10^9	-8.688923174×10^8	-1.778764760×10^8

$$Q^{(3)} = \frac{8 - 15\eta + 192Q^{(0)} \left\{ 2 - \eta \left[53 + 280Q^{(0)}(3 - 10\eta)^2 - 100\eta \right] \right\}}{8(1 - \eta)^2} \quad (33)$$

Insertion of Eqs. (31)–(33) into Eq. (21) with $m = 1$ leads to the quartic equation

$$8 - 15\eta + 192Q^{(0)} \left\{ 2 - \eta \left\{ 88 - 135\eta + 1960Q^{(0)} \left[3 - 4\eta \left[9 - 10\eta + 240Q^{(0)}(1 - \eta) \right] \right] \right\} \right\} \times \left(3 - 10\eta \left(1 - 84Q^{(0)}(1 - \eta) \right) \right) \right\} = 0. \quad (34)$$

In the interval $0.446469 \lesssim \eta < 1$ the four roots are real. On the other hand, for $0 \leq \eta \lesssim 0.446469$ two of the roots become complex conjugates and only two roots remain real, the physical one being finite in the limit $\eta \rightarrow 0$. Although an explicit expression exists for the physical root of Eq. (34), it is of course too cumbersome and will be omitted here. Such an expression involves the term $[P_4(\eta)P_6(\eta)]^{1/2}$, where $P_4(\eta) = 1 + 94\eta + 202\eta^2 + \frac{1360}{3}\eta^3 + 50\eta^4$ and $P_6(\eta) = 1 + 99\eta - \frac{307}{8}\eta^2 - \frac{339}{4}\eta^3 - \frac{2762}{3}\eta^4 + \frac{695}{2}\eta^5 + \frac{5575}{108}\eta^6$. As a consequence, $Q^{(0)}$ (and hence $Q^{(m)}$ and Q_m) possesses branch points at the zeroes of $P_4(\eta)$ and $P_6(\eta)$. The zero of $P_4(\eta)$ closest to the origin is $\eta'_{\text{branch}} \simeq -0.0108868$, while that of $P_6(\eta)$ is $\eta_{\text{branch}} \simeq -0.0100625$. Consequently, the series expansion of Q_m in powers of η converges for $\eta < \eta_{\text{conv}}^{\text{PY}} \simeq 0.0100625$. Therefore, this is the radius of convergence of the virial series for a seven-dimensional hard-sphere fluid described by the PY approximation.

Table I shows the first few coefficients $Q_{m,n}$. The exact values are rational numbers, but they become more and more involved as the order n increases and so they are expressed in real form in Table I. From Eq. (29) we can obtain the virial coefficients corresponding to the virial and the compressibility routes. The first few values are listed in Table II. Table II also gives the known exact values^{25,26} $B_n^{\text{ex}}/B_2^{n-1}$, as well as the CS-like values $B_n^{\text{CS}}/B_2^{n-1}$, where $B_n^{\text{CS}} = \alpha B_n^{\text{PY-c}} + (1 - \alpha)B_n^{\text{PY-v}}$ with the simple choice $\alpha = \frac{5}{6}$. Note that the choice $\alpha \simeq 0.6$ would make $B_4^{\text{CS}} \simeq B_4^{\text{ex}}$, whereas the choice $\alpha \simeq 0.7$ would make $B_5^{\text{CS}} \simeq B_5^{\text{ex}}$ and $B_6^{\text{CS}} \simeq B_6^{\text{ex}}$. However, comparison with molecular dynamics simulations (see Section III) favors $\alpha \simeq 0.8$.

From Table II we observe that the virial route of the PY approximation incorrectly yields a negative value for the fourth virial coefficient (which actually becomes negative for $d \geq 8$,^{24,25,26}) while the compressibility route predicts the correct sign.³¹ We have computed $B_n^{\text{PY-v}}$ and $B_n^{\text{PY-c}}$ for values of n much larger than those displayed in Table II. The results indicate that $\text{sgn}(B_n^{\text{PY-v}}) = (-1)^{n+1}$ for $5 \leq n \leq 97$ but $\text{sgn}(B_n^{\text{PY-v}}) = (-1)^n$ for $n \geq 98$; analogously, $\text{sgn}(B_n^{\text{PY-c}}) = (-1)^{n+1}$ for $5 \leq n \leq 80$ but $\text{sgn}(B_n^{\text{PY-c}}) = (-1)^n$ for $n \geq 81$. Therefore, both routes synchronize their signs for $5 \leq n \leq 80$ and again for $n \geq 98$. This peculiar behavior of the alternating character of the virial series seems to be a consequence of the proximity between the two branch point singularities closest to the origin, $\eta_{\text{branch}} \simeq -0.0100625$ and $\eta'_{\text{branch}} \simeq -0.0108868$, both located on the negative real axis. To confirm this interpretation, we plot in Fig. 1 the ratios $|b_n^{\text{PY-v}}/b_{n+1}^{\text{PY-v}}|$, $|b_n^{\text{PY-c}}/b_{n+1}^{\text{PY-c}}|$, and $|b_n^{\text{CS}}/b_{n+1}^{\text{CS}}|$. Recall that the radius of convergence of the virial series is $\eta_{\text{conv}} = \lim_{n \rightarrow \infty} |b_n/b_{n+1}|$. Figure 1 shows that for $n \lesssim 50$ the ratio $|b_n/b_{n+1}|$ seems to converge from above to the *apparent* radius of convergence $\eta'_{\text{conv}} = -\eta'_{\text{branch}} \simeq 0.0108868$. However, the true radius $\eta_{\text{conv}}^{\text{PY}} = -\eta_{\text{branch}} \simeq 0.0100625$ is reached from below for $n \gtrsim 100$.

As mentioned in Sec. I, the radius of convergence predicted by the PY approximation in the five-dimensional case is $\eta_{\text{conv}}^{\text{PY}} \simeq 0.0566243$. When going to the next odd dimensionality, the radius of convergence has shrunk to $\eta_{\text{conv}}^{\text{PY}} \simeq 0.0100625$. In terms of the scaled density per dimension introduced by Frisch and Percus,¹⁵ the radius of convergence is $\hat{\rho}_{\text{conv}}^{\text{PY}} \simeq 1.126$ for $d = 5$ and $\hat{\rho}_{\text{conv}}^{\text{PY}} \simeq 1.037$ for $d = 7$. Therefore, it nicely tends to converge to the expected value $\hat{\rho}_{\text{conv}} = 1$ as $d \rightarrow \infty$. In addition, the PY value of $\eta_{\text{conv}} = 2^{1-d} B_2 \lim_{n \rightarrow \infty} |B_n/B_{n+1}|$ for $d = 7$ is consistent with estimates obtained from Table XVIII of Ref. 25. By assuming that the Ree–Hoover ring diagrams

TABLE II: Values of B_n/B_2^{n-1} for $n = 3-8$, according to the virial route of the PY approximation, the compressibility route of the PY approximation, the CS-like approximation (15) with $\alpha = \frac{5}{6}$, and the known exact results.^{25,26}

n	$B_n^{\text{PY-v}}/B_2^{n-1}$	$B_n^{\text{PY-c}}/B_2^{n-1}$	$B_n^{\text{CS}}/B_2^{n-1}$	$B_n^{\text{ex}}/B_2^{n-1}$
3	0.2822265625	0.2822265625	0.2822265625	0.2822265625
4	$-7.499694824 \times 10^{-3}$	$2.155081431 \times 10^{-2}$	$1.670906279 \times 10^{-2}$	$9.873(4) \times 10^{-3}$
5	$1.235022893 \times 10^{-2}$	$5.116807918 \times 10^{-3}$	$6.322378086 \times 10^{-3}$	$7.071(7) \times 10^{-3}$
6	$-8.177005666 \times 10^{-3}$	$-1.865328120 \times 10^{-3}$	$-2.917274378 \times 10^{-3}$	$-3.52(2) \times 10^{-3}$
7	$6.553131160 \times 10^{-3}$	$1.384246670 \times 10^{-3}$	$2.245727418 \times 10^{-3}$	
8	$-5.762797816 \times 10^{-3}$	$-1.078783146 \times 10^{-3}$	$-1.859452258 \times 10^{-3}$	

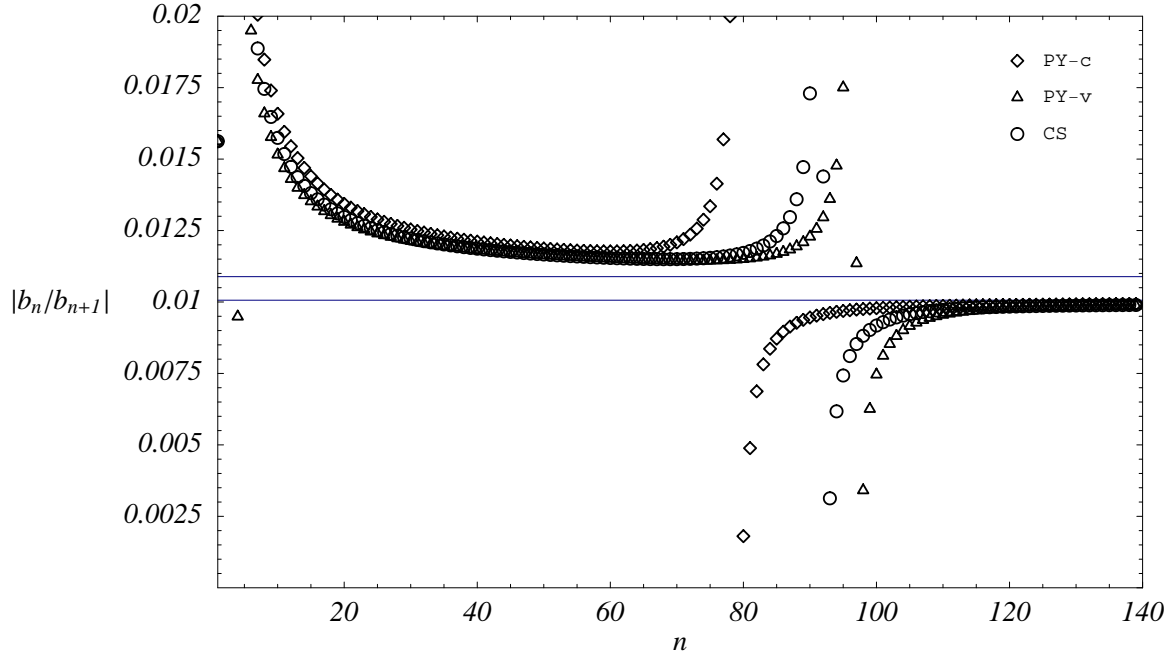


FIG. 1: Plot of the ratios $|b_n^{\text{PY-c}}/b_{n+1}^{\text{PY-c}}|$ (diamonds), $|b_n^{\text{PY-v}}/b_{n+1}^{\text{PY-v}}|$ (triangles), and $|b_n^{\text{CS}}/b_{n+1}^{\text{CS}}|$ (circles). The horizontal lines correspond to the apparent radius of convergence $\eta'_{\text{conv}} \simeq 0.0108868$ and to the true radius of convergence $\eta_{\text{conv}}^{\text{PY}} \simeq 0.0100625$.

dominate for high d ,²⁵ one has $\eta_{\text{conv}} < 2^{-6} B_2 |B_9/B_{10}| \approx 2^{-6} 0.0132/0.0143 \simeq 0.014$ for $d = 7$, which agrees with the PY value $\eta_{\text{conv}}^{\text{PY}} \simeq 0.0100625$. Clisby and McCoy's estimate²⁵ $\eta_{\text{conv}} \simeq 0.052$ for $d = 5$ is also close to the PY value $\eta_{\text{conv}}^{\text{PY}} \simeq 0.0566243$. All of this leads us to conjecture that the PY solution gives a fair estimate of the radius of convergence of the true virial series for high dimensionalities. Pushing this conjecture even further, we can expect the true radius of convergence to be due to a singularity (pole or branch point) located on the negative real axis, so that the virial coefficients alternate in sign beyond a certain order. Figure 2 shows the virial coefficients $B_n^{\text{PY-v}}/B_2^{n-1}$, $B_n^{\text{PY-c}}/B_2^{n-1}$, and $B_n^{\text{CS}}/B_2^{n-1}$ in the seven-dimensional case. In the spirit of the above conjecture, one may speculate that the exact values of B_n/B_2^{n-1} lie in between $B_n^{\text{PY-v}}/B_2^{n-1}$ and $B_n^{\text{PY-c}}/B_2^{n-1}$, perhaps not far from the interpolated values $B_n^{\text{CS}}/B_2^{n-1}$. The reduced virial coefficients B_n/B_2^{n-1} start decreasing in magnitude, reach a minimum around $n = 10$, and then grow with n . The fact that the PY solution in the three-dimensional case does not possess a branch point singularity, so that all the virial coefficients remain positive, casts some doubts as to whether the true virial series fails to converge for densities close to the freezing density $\eta_f \simeq 0.494$. In any case, the true radius of convergence for $d = 3$ cannot be larger than the crystalline close-packing value $\eta_{\text{cp}} = \pi\sqrt{2}/6 \simeq 0.7405$, while the PY solution has $\eta_{\text{conv}}^{\text{PY}} = 1$.

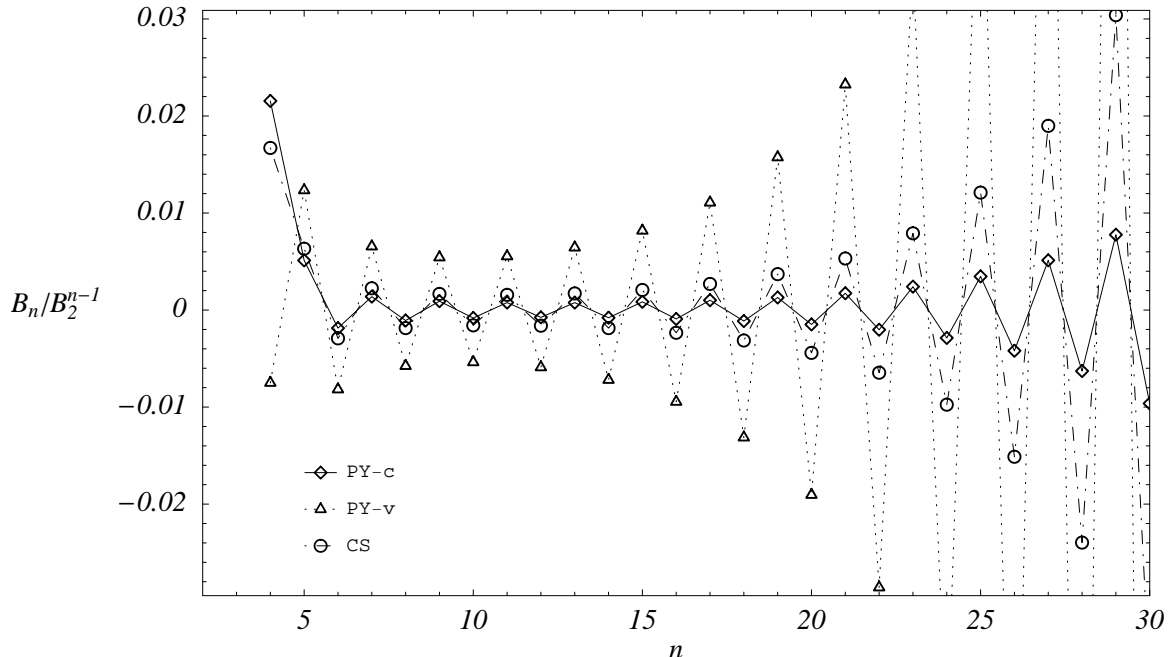


FIG. 2: Plot of the virial coefficients $B_n^{\text{PY-c}}/B_2^{n-1}$ (diamonds), $B_n^{\text{PY-v}}/B_2^{n-1}$ (triangles), and $B_n^{\text{CS}}/B_2^{n-1}$ (circles).

III. MOLECULAR DYNAMICS SIMULATIONS

A. Method

The numerical simulation was implemented by using the same algorithm as described in Ref. 21, which is also based on the work of Michels and Trappeniers⁵ for four- and five-dimensional hyperspheres.

For our simulations, in order to keep the computing time within reasonable limits and at the same time being able to examine a wide density range, the initial configuration is chosen to be the one obtained by placing $N = 64$ hyperspheres in a unitary cell of a d -type lattice. The simulation cell is a hypercube of side L and volume $V = L^d = N/\rho$ and the minimum image convention and periodic boundary conditions in all directions have been applied, in the same way as in the 3D case.³²

During the simulations only binary collisions are taken into account, while collisions between three or four particles are ignored. The collision time for every pair of particles is calculated and the the smallest value is obtained. All the particles are moved during this time at constant velocity. The pair of particles that suffers a collision is treated according to impulsive dynamics and the velocities are changed; in this step the hard collisional virial is calculated. This allows one to evaluate the excess compressibility factor as

$$Z - 1 = -\frac{1}{N\langle v^2 \rangle \Delta t} \sum_{ij} \mathbf{r}_{ij} \cdot \Delta \mathbf{v}_i, \quad (35)$$

where $\langle v^2 \rangle$ is the mean square velocity, Δt is the simulated time, \mathbf{r}_{ij} is the relative position vector between colliding particles i and j , and $\Delta \mathbf{v}_i$ the change in velocity of the particle i on collision.

The program used has been previously validated for $d = 4$ and $d = 5$, reproducing the excess compressibility factor obtained by Michels and Trappeniers.⁵

The equation of state is achieved by changing the diameter σ of the particles, in such a way that the reduced density $\rho^* = \rho\sigma^d$ changes, and letting the system to relax up to an equilibrium pressure. The errors associated with our calculation were computed following standard methods for errors in equilibrium averages.³²

TABLE III: Compressibility factor as a function of η for different approximations and simulation data.

η	Z_{simul}	Z_{CS}	$Z_{\text{PY-v}}$	$Z_{\text{PY-c}}$	$Z_{[4,0]}$	$Z_{[2,2]}$	$Z_{[3,2]}$	$Z_{[2,0]}^{\text{BC}}$	$Z_{[2,2]}^{\text{MSAV}}$	Z_{SMS}	Z_{LM}
0.0037	1.25366(2)	1.25223	1.25192	1.25229	1.25214	1.25214	1.25214	1.25233	1.25214	1.25233	1.25217
0.0074	1.5337(1)	1.53751	1.53516	1.53797	1.53687	1.53687	1.53681	1.53829	1.53685	1.53827	1.53725
0.0111	1.8646(3)	1.85767	1.84997	1.85921	1.85577	1.85576	1.85534	1.86008	1.85562	1.86003	1.85745
0.0148	2.2103(3)	2.21482	2.19691	2.21840	2.21093	2.21094	2.20930	2.22006	2.21033	2.21993	2.21565
0.0185	2.6174(2)	2.61124	2.57674	2.61814	2.60499	2.60513	2.60047	2.62071	2.60328	2.62047	2.61524
0.0221	3.0650(4)	3.04946	2.99039	3.06128	3.04111	3.04170	3.03080	3.06467	3.03716	3.06423	3.0600
0.0258	3.5449(5)	3.53219	3.43890	3.55085	3.52298	3.52481	3.50243	3.55469	3.51502	3.55399	3.55394
0.0295	4.0989(7)	4.06234	3.92342	4.09012	4.05480	4.05948	4.01769	4.09372	4.04037	4.09264	4.10109
0.0332	4.7013(5)	4.64302	4.44519	4.68258	4.64133	4.65183	4.57911	4.68483	4.61713	4.68326	4.70519
0.0369	5.389(1)	5.27757	5.00555	5.33198	5.28785	5.30924	5.18944	5.33130	5.24971	5.32910	5.36929
0.0406	6.051(1)	5.96955	5.60592	6.04228	6.00015	6.04073	5.85164	6.03659	5.94307	6.03358	6.09511
0.0443	6.8179(6)	6.72276	6.24777	6.81775	6.78456	6.85731	6.56896	6.80433	6.70273	6.80033	6.88228
0.0480	7.6325(1)	7.54121	6.93269	7.66292	7.64794	7.77255	7.34490	7.63837	7.53489	7.63317	7.72727
0.0517	8.5133(2)	8.42922	7.66233	8.58259	8.59769	8.80333	8.18328	8.54278	8.44645	8.53613	8.62220
0.0554	9.4294(3)	9.39134	8.43841	9.58192	9.64172	9.97083	9.08829	9.52186	9.44519	9.51348	9.55355
0.0591	10.492(1)	10.4324	9.26275	10.6664	10.7885	11.3020	10.0645	10.5801	10.5398	10.5697	10.5009
0.0628	11.570(3)	11.5577	10.1372	11.8417	12.0469	12.8317	11.1168	11.7224	11.7400	11.7096	11.4365
0.0664	12.694(1)	12.7725	11.0638	13.1142	13.4266	14.6056	12.2507	12.9537	13.0569	12.9381	12.3252
0.0701	13.907(3)	14.0828	12.0446	14.4904	14.9374	16.6847	13.4722	14.2794	14.5029	14.2607	13.1265
0.0720	9.03944(6)	14.7756	12.5559	15.2196	15.7454	17.8637	14.1178	14.9794	15.2786	14.9589	13.4810

B. Results

We have computed the compressibility factor for densities $0.1 \leq \rho^* \leq 1.90$ with a step $\Delta\rho^* = 0.1$, as well as for $\rho^* = 1.95$. The simulation data obtained by our molecular dynamics simulations are listed in Table III. At the largest density $\rho^* = 1.95$ ($\eta = 0.0720$) the compressibility factor presents a dramatic drop. We interpret this as an indication of the freezing transition. Consequently, the density at which the seven-dimensional fluid of hard spheres freezes can be estimated as $\rho_f^* \lesssim 1.95$ or, equivalently, $\eta_f \lesssim 0.072$. From Fig. 5 of Ref. 22 one can observe that $\ln \eta_f(d)$ is almost a linear function of the dimensionality d , with a slight negative curvature. According to this, knowing the freezing densities $\eta_f(d)$ and $\eta_f(d+2)$, one can estimate the freezing density $\eta_f(d+4)$ as $\eta_f(d+4) \lesssim \eta_f^2(d+2)/\eta_f(d)$. Given that $\eta_f(3) \simeq 0.494$ and $\eta_f(5) \simeq 0.19$, one has $\eta_f(7) \lesssim 0.19^2/0.494 \simeq 0.073$, in close agreement with our estimate. An independent estimate based on a conjecture by Colot and Baus⁶ confirms again this value. These authors suggested that the ratio of length scales $[\eta_f(d)/\eta_{\text{cp}}(d)]^{1/d}$ is practically independent of d , so that $\eta_f(d+2) \simeq \eta_{\text{cp}}(d+2)[\eta_f(d)/\eta_{\text{cp}}(d)]^{(d+2)/d}$. The general expression for the close-packing fraction $\eta_{\text{cp}}(d)$ is not known, but for $d < 25$ the values are not far from Blichfeldt's upper estimate²² $\eta_{\text{cp}}(d) \leq 2^{-d/2}(d+2)/2$. Using $\eta_f(5) \simeq 0.19$, we get $\eta_f(7) \simeq 0.076$, which is again consistent with our estimate.

Table III also gives some theoretical values: the PY predictions $Z_{\text{PY-v}}$ and $Z_{\text{PY-c}}$, the CS-like interpolation (15) with $\alpha = \frac{5}{6}$, the truncated virial expansion $Z_{[4,0]}$, the Padé approximants $Z_{[2,2]}$ and $Z_{[3,2]}$ [the three latter being obvious extensions of the approximations (8)–(10)], the rescaled virial expansion $Z_{[2,0]}^{\text{BC}}$ defined by Eq. (11), the rescaled Padé approximant $Z_{[2,2]}^{\text{MSAV}}$ defined by a natural extension of Eq. (12), the SMS approximation (13), and the LM proposal (14).

Although the knowledge of the sixth virial coefficient B_6 would allow one to consider the truncated series $Z_{[5,0]}$, it is not included in Table III because it turns out to be clearly inferior to $Z_{[4,0]}$. This is a consequence of the fact that $B_6 < 0$, so that $Z_{[5,0]} < Z_{[4,0]}$, while for small and moderate densities $Z_{[4,0]} < Z_{\text{simul}}$. This is a strong indication that the unknown seventh virial coefficient B_7 must be positive. Among the different Padé approximants that can be constructed from the knowledge of the first six virial coefficients, the best agreement with the simulation data is presented by $Z_{[2,2]}$ for $\rho^* \lesssim 1.4$ ($\eta \lesssim 0.0517$) and by $Z_{[3,2]}$ for $\rho^* \gtrsim 1.4$ ($\eta \gtrsim 0.0517$). It is interesting to note that both Padé approximants have poles on the negative real axis (at $\eta \simeq -0.079$ in the case of $Z_{[2,2]}$ and at $\eta \simeq -0.025$ in the case of $Z_{[3,2]}$), so that the extrapolated virial coefficients have alternating signs. Paradoxically, while the rescaled expansion $Z_{[2,0]}^{\text{BC}}$ incorporates the first three virial coefficients only, it exhibits a better agreement with simulation than those rescaled expansions that can be constructed with the first four, five, or six virial coefficients, so the latter are not included in Table III. Analogously, the best performance among the rescaled Padé approximants corresponds to $Z_{[2,2]}^{\text{MSAV}}$. Interestingly, the SMS proposal [cf. Eq. (13)] and the approximation $Z_{[2,0]}^{\text{BC}}$ yield practically equivalent

results. The difference between both EOS is

$$Z_{[2,0]}^{\text{BC}}(\eta) - Z_{\text{SMS}}(\eta) = \frac{\eta^3}{(1-\eta)^7} (35 - 35\eta + 21\eta^2 - 7\eta^3 + \eta^4). \quad (36)$$

This corresponds to a relative difference smaller than 0.14% for the density range considered in the simulations.

Two of the theoretical EOS included in Table III, namely Z_{CS} and Z_{LM} , have an empirical character. The proposal (15) is based on the observation that the two PY routes tend to bracket the simulation data, as happens in the three-dimensional³⁰ and five-dimensional¹⁷ cases. We have found that the value $\alpha = \frac{5}{6}$ of the parameter is the simplest rational number that makes Z_{CS} reproduce fairly well the simulation values. In the case of the Luban–Michels EOS (14) one fits $\zeta(\eta)$ to a linear function. Figure 3 shows the simulation values of $\zeta(\eta)$. As in the five-dimensional case,¹¹ $\zeta(\eta)$ is an increasing function of η , while it is a decreasing function for $d = 2-4$. A linear fit in the interval $0.5 \leq \rho^* \leq 1.9$ ($0.0185 \leq \eta \leq 0.0701$) yields

$$\zeta(\eta) = -5.81 + 88.2\eta. \quad (37)$$

The column labeled Z_{LM} in Table III has been evaluated using the fit (37). On the other hand, our simulation data seem to indicate a negative curvature of $\zeta(\eta)$.

Table III shows that up to $\rho^* = 0.8$ ($\eta = 0.0295$) all the different theoretical results tabulated, including the simple truncated virial expansion $Z_{[4,0]}$, behave relatively well. For larger densities, $Z_{[4,0]}$ tends to overestimate the simulation data, while the Padé approximants $Z_{[2,2]}^{\text{BC}}$ and $Z_{[3,2]}$ tend to underestimate them. The best global agreement is presented by Z_{CS} , Z_{LM} , $Z_{[2,0]}^{\text{BC}}$, and Z_{SMS} . This is especially noteworthy in the case of the two latter approximations, since they do not contain fitting parameters and, moreover, only the knowledge of the first three virial coefficients is exploited. This contrasts with Z_{LM} , which includes the fourth virial coefficient and contains two fitting parameters. On the other hand, Z_{CS} belongs in a different class of approximations. Given the involved algebraic structure of the PY solution, Z_{CS} does not intend to represent a practical recipe to the EOS of a seven-dimensional hard-sphere fluid. Instead, its role is to highlight the fact that the two PY routes keep bracketing the simulation data, so that an interpolation between them with a density-independent parameter α is rather accurate, as graphically illustrated in Fig. 4. This gives some confidence on the expectation that some of the analytical properties of the PY solution (e.g., alternating character of the virial series, branch points located on the negative real axis, ...) may shed light on the true behavior of the exact series.

IV. DISCUSSION

The results of the previous sections deserve further discussion. To begin with, to our knowledge this is the first time that a molecular dynamics simulation has been carried out on a seven-dimensional hard-sphere fluid. The simulation strategy that we adopted implied a compromise between computer process time and density range to be explored and the outcome is rather encouraging. The availability of simulation data for the EOS of the fluid allowed us to locate the freezing transition and also to assess the merits and limitations of various proposals that have been made in the literature for the compressibility factor of hard hyperspheres. From this analysis it is clear that even simple approximations such as the $Z_{[2,0]}^{\text{BC}}$ and Z_{SMS} do a reasonably good job and that, as it occurs in other dimensionalities, the virial and compressibility routes to the EOS in the PY approximation keep bracketing the simulation data, so that a Carnahan–Starling-like recipe of the form of Eq. (15) turns out to be rather accurate. However the parameter α seems not to follow a simple relation as the ones suggested by González et al.¹² or Santos.¹⁷

We also presented the analytical solution of the PY equation for a hard-sphere fluid in 7D. Out of the analytical solutions of the PY equation in odd dimensions, this is the only one that had not been explicitly written down up to now. Such a solution allowed us to carry out an analysis of the virial coefficients arising both in the virial and in the compressibility routes and to determine the radius of convergence of both virial series. The results indicate some peculiar behavior of the virial coefficients with the virial route incorrectly predicting a negative fourth virial coefficient. The radius of convergence of the virial series is due to a singularity (branch point) located on the negative real axis and therefore what one has is an alternating series. Because of the good agreement between our value of the radius of convergence of the virial series and other independent estimates and the similar results obtained for $d = 5$, it is tempting to conjecture that the PY solution for even higher dimensionalities should provide a rather accurate estimate of the radius of convergence of the true virial series and that it is the existence of singularities on the negative real axis (either poles or branch points) which determines such radius.

As a final point it is worth commenting that in this case our analysis was facilitated by the fact that we could combine both the analytical and the simulation results. And due to the common features such as the freezing transition that hard-core systems in different dimensionalities share, the expectation and the hope is that the present results shed some more light on the thermodynamic properties of such systems.

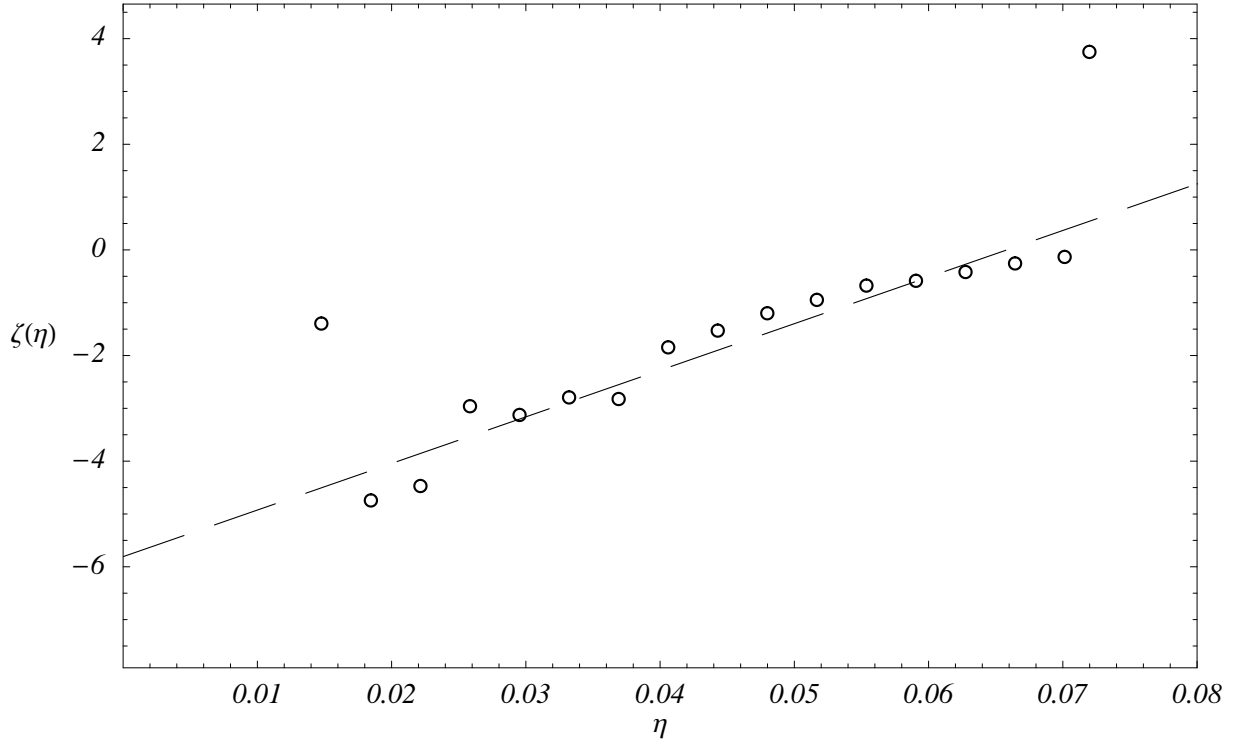


FIG. 3: Plot of the simulation values of the function $\zeta(\eta)$ defined by Eq. (14). The dashed line is the linear fit (37).

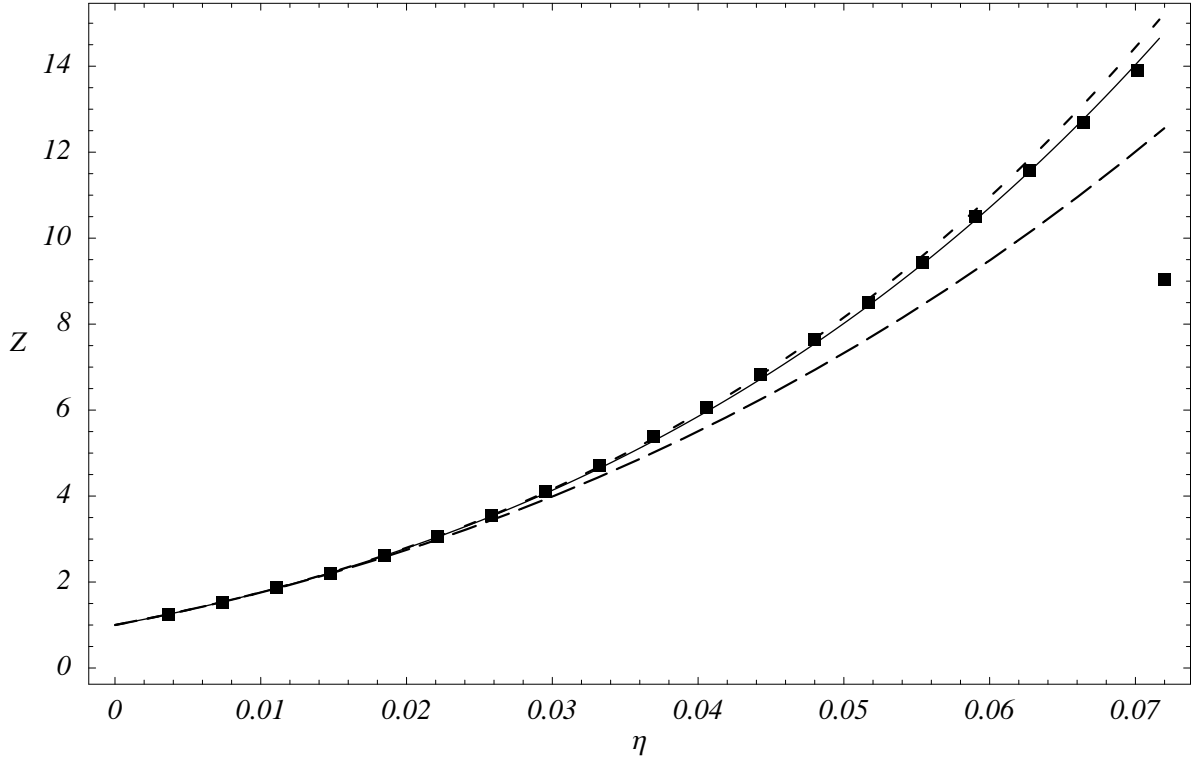


FIG. 4: Compressibility factor as a function of the packing fraction. The squares represent simulation data, the dash line represents Z_{PY-c} , the dash-dotted line represents Z_{PY-v} , and the solid line represents the CS-like interpolation (15) with $\alpha = \frac{5}{6}$.

Acknowledgments

M.R. acknowledges the financial support of CONACyT through project No. I38644-E. The research of A.S. has been partially supported by the Ministerio de Ciencia y Tecnología (Spain) through grant No. BFM2001-0718.

-
- * mrp@cie.unam.mx
 † malopez@servidor.unam.mx
 ‡ andres@unex.es; <http://www.unex.es/fisteor/andres/>
- ¹ C. Freasier and D. J. Isbister, *Mol. Phys.* **42**, 927 (1981).
 - ² M. Luban and A. Baram, *J. Chem. Phys.* **76**, 3233 (1982).
 - ³ C. G. Joslin, *J. Chem. Phys.* **77**, 2701 (1982).
 - ⁴ E. Leutheusser, *Physica A* **127**, 667 (1984).
 - ⁵ J. P. J. Michels and N. J. Trappeniers, *Phys. Lett. A* **104**, 425 (1984).
 - ⁶ J. L. Colot and M. Baus, *Phys. Lett. A* **119**, 135 (1986).
 - ⁷ M. Baus and J. L. Colot, *Phys. Rev. A* **36**, 3912 (1987).
 - ⁸ Y. Song, E. A. Mason, and R. M. Stratt, *J. Phys. Chem.* **93**, 6916 (1989).
 - ⁹ J. Amorós, J. R. Solana, and E. Villar, *Phys. Chem. Liq.* **19**, 119 (1989).
 - ¹⁰ Y. Song and E. A. Mason, *J. Chem. Phys.* **93**, 686 (1990).
 - ¹¹ M. Luban and J. P. J. Michels, *Phys. Rev. A* **41**, 6796 (1990).
 - ¹² D. J. González, L. E. González, and M. Silbert, *Mol. Phys.* **74**, 613 (1991).
 - ¹³ M. J. Maeso, J. R. Solana, J. Amorós, and E. Villar, *Mater. Chem. Phys.* **30**, 39 (1991).
 - ¹⁴ E. Velasco, L. Mederos, and G. Navascués, *Mol. Phys.* **97**, 1273 (1999).
 - ¹⁵ H. L. Frisch and J. K. Percus, *Phys. Rev. E* **60**, 2942 (1999).
 - ¹⁶ M. Bishop, A. Masters, and J. H. R. Clarke, *J. Chem. Phys.* **110**, 11449 (1999).
 - ¹⁷ A. Santos, *J. Chem. Phys.* **112**, 10680 (2000).
 - ¹⁸ S. B. Yuste, A. Santos, and M. López de Haro, *Europhys. Lett.* **52**, 158 (2000).
 - ¹⁹ G. Parisi and F. Slanina, *Phys. Rev. E* **62**, 6554 (2000).
 - ²⁰ A. Santos, S. B. Yuste, and M. López de Haro, *Mol. Phys.* **99**, 1959 (2001).
 - ²¹ M. González-Melchor, J. Alejandre, and M. López de Haro, *J. Chem. Phys.* **114**, 4905 (2001).
 - ²² R. Finken, M. Schmidt, and H. Löwen, *Phys. Rev. E* **65**, 016108 (2002).
 - ²³ E. Enciso, N. G. Almarza, M. A. González, and F. J. Bermejo, *Mol. Phys.* **100**, 1941 (2002).
 - ²⁴ N. Clisby and B. M. McCoy, *Analytic calculation of B_4 for hard spheres in even dimensions*, cond-mat/0303198 (2003).
 - ²⁵ N. Clisby and B. M. McCoy, *Negative virial coefficients and the dominance of loose packed diagrams for D -dimensional hard spheres*, cond-mat/0303100 (2003).
 - ²⁶ N. Clisby and B. M. McCoy, *New results for the virial coefficients of D -dimensional hard spheres*, cond-mat/0303101 (2003).
 - ²⁷ J. P. Hansen and I. R. McDonald, *Theory of Simple Liquids* (Academic Press, London, 1986).
 - ²⁸ In the notation of Ref. 19, $\ln \hat{\rho}^2 \rightarrow \rho_1 = d^{-1} \ln \bar{\rho}^2$, $\kappa \rightarrow \hat{\rho}_c$, $\hat{\rho}^{2d} \Delta \rightarrow P_c = \exp(dP_1/2)$, and $P_1 = 2 - 2 \ln 2 + \ln \hat{\rho}_c^2$.
 - ²⁹ In their paper,¹⁹ Parisi and Slanina do not locate the breakdown of Eq. (3) at $\hat{\rho} = \hat{\rho}_0$, but at a smaller value $\hat{\rho} = \hat{\rho}'_0 = \left[e/2 + \sqrt{(e/2)^2 - 1} \right]^{1/2} \exp \left[-\sqrt{1 - (2/e)^2}/2 \right] \simeq 1.07614$. This value, which corresponds to $\kappa = 2/e$, is the density beyond which $\hat{\rho}^{2d} \Delta(\hat{\rho})$ diverges. The quantity $\hat{\rho}^{2d} \Delta(\hat{\rho})$ is the *absolute* correction to the *pressure*: $p \propto \hat{\rho}^d + \frac{1}{2} \hat{\rho}^{2d} + \hat{\rho}^{2d} \Delta(\hat{\rho})$. However, since the second virial term $\hat{\rho}^{2d}$ diverges as well in that limit, the relevant behavior is that of the *relative* correction $\Delta(\hat{\rho})$, which diverges at $\hat{\rho} = \hat{\rho}_0$.
 - ³⁰ N. F. Carnahan and K. E. Starling, *J. Chem. Phys.* **51**, 635 (1969).
 - ³¹ As mentioned in Section I, a similar situation takes place with the PY solution for $d = 5$, where $B_6^{\text{PY-v}} < 0$ but $B_6^{\text{PY-c}} > 0$.
 - ³² M. P. Allen and D. J. Tildesley, *Computer Simulation of Liquids* (Clarendon, Oxford, 1987).